Received: 1 August 2024 | Revised: 29 October 2024 | Accepted: 30 November 2024

DOI: 10.1111/php.14050

RESEARCH ARTICLE

520 nm and 660 nm light-emitting diodes modulates pancreatic development and beta cell functions in zebrafish embryos

Ünsal Veli Üstündağ[1,2] | **İsmail Ünal**[3] | **Derya Cansız**[3] | **Merih Beler**[4] | **Naveen Krishna Kanagaraj**[5] | **Amrish Rajendra Kumar**[5] | **Ravindra Peravali**[5] | **Ebru Emekli-Alturfan**[4]

[1]Department of Medical Biochemistry, Faculty of Medicine, Istanbul Atlas University, Istanbul, Turkey

[2]Department of Biochemistry, Institute of Health Sciences, Marmara University, Istanbul, Turkey

[3]Department of Medical Biochemistry, Faculty of Medicine, Istanbul Medipol University, Istanbul, Turkey

[4]Department of Basic Medical Sciences, Faculty of Dentistry, Marmara University, Istanbul, Turkey

[5]Institute of Biological and Chemical Systems, Karlsruhe Institute of Technology, Karlsruhe, Germany

Correspondence
Ünsal Veli Üstündağ, Department of Medical Biochemistry, Faculty of Medicine, Istanbul Atlas University, Istanbul, Turkey.
Email: uvustundag@yahoo.com

Funding information
Scientific and Technological Research Council of Türkiye (TÜBİTAK) 2214A Program; Scientific Research Projects Foundation (BAP) of the Marmara University, Grant/Award Number: TDK-2021-10172

Abstract

Green and Red LEDs increase insulin production, but their comparative effects on pancreatic and beta cell development are unclear. Zebrafish embryos were divided into three groups: Control ($n = 60$), Green (G) ($n = 60$), and Red (R) ($n = 60$), then irradiated for three days (14 hours/day) with 0.5 W/cm^2 G (λpeak = 520 nm, 180 mA) and R (λpeak = 660 nm, 210 mA). At the end of 72 h, pancreatic and beta cells, circadian rhythm, and oxidative stress gene were analyzed using RT-PCR. Malondialdehyde, nitric oxide, superoxide dismutase, and glutathione levels were also evaluated. In the Red group, pancreatic area increased by ~97.13% compared to the Control group and by approximately ~62.16% compared to the G group (both $p < 0.0001$), and no significant difference in beta cell area ($p = 0.964$). G group insulin expression increased 2.31-fold compared to R group ($p < 0.0001$). Red LED treatment increased MDA levels ($p < 0.001$), oxidative stress (*fth1b*, *nqo1*) ($p < 0.0001$), and *per1b* during the photophase ($p < 0.0001$) compared to G group. R LED treatment increases oxidative stress and disrupts circadian rhythm, leading to reduced insulin secretion. The positive effects of G LED treatment have potential for metabolic syndrome, diabetes, and pancreatic diseases.

KEYWORDS

light emitting diode, pancreas, beta cell, insulin, zebrafish

Abbreviations: annat2, Arylalkylamine N-acetyltransferase 2; bcl2, B cell lymphoma 2; bmal1, Brain and Muscle Arnt-Like Protein 1; clock1a, Circadian Locomotor Output Cycles Kaput; cox, Cytochrome C Oxidas; fth1b, Ferritin Heavy Chain 1B; hmox1a, Heme Oxygenase 1A; hnf1a, Hepatocyte Nuclear Factor 1 Alpha; kcnj11, Potassium Channel, Inwardly Rectifing Subfamily J Memeber 11; nkx6.1, Homeobox Protein NKX-6.1; nqo1, NAD(P)H Quinone Dehydrogenase 1; pax4, Paired Box 4; pdx1, Pancreatic Duodenal Homeobox 1; per1b, Period 1B; slc2a2, Solute Carrier Family 2 Member 2; txnrd1, Thioredoxin Reductase 1.

INTRODUCTION

Photobiomodulation (PBM) is a promising approach aimed at enhancing tissue healing and function by regulating cellular metabolism, energy balance, and oxidative stress. Green (G) and Red (R) LED therapies may offer new non-invasive treatment pathways for metabolic disorders by exerting different effects on pancreatic development, insulin signaling, and circadian rhythm. These methods are free from the toxic side effects of chemicals, providing low-cost solutions with rapid healing times, which can reduce healthcare expenses. Furthermore, they may improve overall health and quality of life by reducing cellular damage and oxidative stress.

LEDs with different wavelengths have been shown to influence cell proliferation, differentiation, angiogenesis, ATP synthesis, oxidative stress responses, regulation of blood sugar levels, glycogen synthesis, and hepatic parameter modulation.[1–6] G and R treatments optimize ATP synthesis by modulating cellular energy production, oxidative stress responses, and circadian rhythms,[2,4] offering potential therapeutic strategies for metabolic diseases, particularly metabolic syndrome and diabetes. While G treatment modulates cellular signaling pathways, especially oxidative stress and inflammatory responses, R treatment promotes energy production and cellular healing by increasing the activity of enzymes such as mitochondrial cytochrome C oxidase.[5,6] The potential of G treatment to alter cellular stress responses by regulating intracellular calcium levels is a significant finding for the photomodulation of secretory cells.[7] Evidence exists that R treatment exerts different effects on the biological clock and metabolic processes by suppressing melatonin production and secretion.[5,8,9] We know that prolonged, dose-dependent exposure to R treatment increases oxidative stress and leads to cellular damage.[8,10]

The lack of understanding regarding the specific sensitivity of pancreatic development, beta cell differentiation, and insulin production to light spectra necessitates a better comprehension of the roles of transcription factors such as PTF1A, PDX1, PAX4, and NKX6.1, which mediate the morphogenetic transformation of pancreatic multipotent cells.[11–14] While *nkx6.1* and *pdx-1* stimulate the differentiation and proliferation of beta cells in the islets, an increase in *ptf1a* expression directs cells toward an acinar cell fate.[14,15] The synthesis and secretion of insulin are regulated by *pdx1* and *mafa, neurod1, nkx6.1, slc2a2, kcnj11*, and glucose uptake in beta cells.[16] GLUT2, encoded by *slc2a2*, is responsible for glucose entry into beta cells.[17] Elevated glucose levels in beta cells activate glycolysis and the pentose phosphate pathway, leading to increased intracellular NADH and NADPH levels, which regulate ATP production and redox reactions of molecules involved in the antioxidant system.[18] The increased ATP levels in beta cells interact with the Kir6.2 protein, encoded by *kcnj11*, which is a component of the K-ATP channel. When intracellular glucose levels rise, ATP closes the K-ATP channel, leading to increased intracellular potassium levels; this depolarizes the cell membrane, opens voltage-dependent calcium channels, and allows calcium to enter the cell, thereby triggering insulin secretion.[19] Although studies on the effects of G and R treatments on pancreatic development and beta cell differentiation are limited, there is cellular evidence that LED can modulate pancreatic and insulin signaling.[7] R treatment increases mitochondrial respiration and ATP production in cells through a mechanism similar to glucose stimulation, resulting in the upregulation of Ca^{2+}/Na^{+} antiporters, Na^{+}/K^{+} ATPase, and Ca^{2+} pumps by enhancing the proton gradient.[7,20] While the potential of G treatment to alter intracellular Ca^{2+} levels and, consequently, cellular stress responses has been previously studied, its effects on insulin synthesis and secretion in beta cells have not been investigated. R (660 nm) treatment enhances energy metabolism by activating cytochrome C oxidase (COX), an enzyme in the mitochondrial respiratory chain, while G (520 nm) treatment affects oxidative stress responses and cellular ion channels.[7] G treatment may increase insulin synthesis and secretion by regulating circadian rhythm and oxidative stress. Although R treatment can enhance mitochondrial energy production, prolonged exposure may lead to oxidative stress and cellular damage. Understanding the potential effects of G and R on the pancreas and beta cells could contribute to the development of new light-based therapeutic strategies for the treatment of diseases such as diabetes and metabolic syndrome.

Sleep–wake behavior, endocrine and metabolic regulation, cellular proliferation, and gene expression are regulated by the positive regulators of the circadian rhythm, BMAL1 and CLOCK (which increase during the photophase), and the negative regulators, PER and CRY (which increase during the skotophase).[21] The expression of circadian transcription factors has been demonstrated in beta cells, and the ablation of the pancreatic circadian cycle has been reported to trigger the onset of diabetes.[22–25] The melatonin hormone secreted by the circadian rhythm suppresses insulin expression.[26] This mechanism helps maintain energy levels during the dark phase. On the other hand, melatonin functions as a scavenger for reactive oxygen species (ROS).[27] In our previous study, we showed that R treatment at 1 watt power led to a decrease in melatonin levels in zebrafish embryos, disrupting the oxidant–antioxidant balance.[8] The ability of G treatment to regulate metabolic processes by maintaining circadian

rhythm paves the way for the development of new approaches in the treatment of diseases such as metabolic syndrome and obesity.[5,6]

Zebrafish embryonic cells become light-sensitive as early as 5 hpf during the gastrula stage. The pineal organ initiates this capability at 24 hpf, and retinal photoreceptors begin to develop between the second and third days of development.[28] This short developmental period and the transparent embryonic development facilitate the assessment of systemic effects of light and the observation of developmental changes in internal organs such as the pancreas. Due to these developmental characteristics, Zebrafish embryos have been selected as the model organism for this study.

The aim of our study was to compare the effects of G (520 nm) and R (660 nm) LED light sources on in vivo pancreatic development and beta cell differentiation. We evaluated pancreatic and beta cell development morphologically and examined the expressions of differentiation-related transcription factor genes, oxidative stress genes, and circadian genes. Additionally, we assessed biochemical levels of malondialdehyde (MDA), nitric oxide (NO), superoxide dismutase (SOD), and glutathione (GSH).

MATERIALS AND METHODS

Experimental design

In this study, the effects of 14 hours/day Green (520 nm, 0.5 watt/m^2) and Red (660 nm, 0.5 watt/m^2) LED light spectra on pancreatic and beta cell development were investigated by applying treatments for 72 h from the zygote stage. The development of the pancreas, insulin synthesis, and gene expression related to circadian rhythms and oxidative stress were evaluated; additionally, biochemical methods were used to analyze levels of MDA, NO, SOD, and GSH.

Zebrafish care and embryo collection

Three different strains of zebrafish, obtained from the Marmara University Zebrafish Resource Center (MZRC) and the European Zebrafish Resource Center (EZRC) at Karlsruhe Institute of Technology, were used in this study. Embryos from AB/AB (wild type) zebrafish obtained from MZRC were used to evaluate gene expressions related to pancreatic development, beta cell development, insulin secretion, circadian rhythms, and oxidative stress. Embryos from the Tg(*ptf1a*:eGFP)jh1 strain obtained from EZRC were utilized to observe pancreatic development, while the Tg(*ins*:mCherry)jh2 strain was used to study beta cell development and insulin secretion, allowing for the collection of quantitative data.

Adult zebrafish were maintained under stable water conditions (pH: 7.2 ± 0.1, Conductivity: 750 ± 50 µS/cm) in an aquarium rack system (Zebtec, Tecniplast, Italy) at a temperature of 27 ± 1°C with a 14/10 hour light/dark cycle. They were fed commercial fish flakes (TetraMin®) and *Artemia nauplii* three times daily. The embryos obtained from adult zebrafish were washed with E3 (5 mmol/L NaCl, 0.33 mmol/L $CaCl_2$, 0.33 mmol/L $MgSO_4 \cdot 7H_2O$, and 0.17 mmol/L KCl) (the same protocol was applied for all three strains) and then divided into three groups in E3 medium.

Since the zebrafish embryos used in this study were less than 5 days old, ethical approval was not required in accordance with the protocols implemented under the Council of Europe Directive 86/609/EEC.[29]

Embryonic LED exposures and investigation of pancreatic morphology

As described by Westerfield,[30] fertilized healthy embryos were randomly assigned into 6 cm glass Petri dishes at the eight-cell stage as follows: Control ($n = 60$), Green (510–530 nm/peak $\lambda = 520$ nm, 180 mA, 0.5 watt/m^2, $n = 60$), and Red (650–670 nm/peak $\lambda = 660$ nm, 210 mA, 0.5 watt/m^2, $n = 60$). The control group consisted of 400 lux white LEDs (3200 K, 0.5 watt/m^2), used to simulate a natural photoperiod (SNP). The spectral ranges and Kelvin values of the LEDs were calibrated using a Sekonic C-700R SpectroMaster light meter (Sekonic).[8] All LED exposure groups were subjected to a photoperiod of 14 h (light phase)/10 h (dark phase) as previously defined[8] (lights turned on at 09:00 am and off at 11:00 pm). Throughout the experimental period (3 days, 72 hours), embryos were incubated at 28°C. Light-blocking photoblock plates were placed between the LED light sources during the experiment. An incubator (Nuve EN400) equipped with a fan system was used to prevent temperature fluctuations. At the end of 72 h, Tg(*ptf1a*:eGFP)jh1 and Tg(*ins*:mCherry)jh2 line embryos were anesthetized with 0.02% Tricaine-Methanesulfonate (MS-222) and photographed using a Leica DMi8 inverted fluorescence microscope in 96-well plates. Subsequently, lysates ($n = 30$) for RT-PCR and homogenates ($n = 30$) for biochemical parameters were prepared. The images were analyzed using ImageJ (open-source software). Fluorescence levels were determined by corrected total cell fluorescence (CTCF) calculated as: integrated density-(area selected × mean fluorescence of the background readings).

Total RNA extraction and cDNA synthesis

Total RNA isolation from 30 embryos in each group at 72 hpf was performed using the RNeasy Mini Kit (Cat No./ID: 74104). For each exposure group ($n = 30$ embryos), diluted RLT buffer was added to the whole body embryos. Following homogenization, samples were centrifuged at 14,000×*g* for 3–5 min. The supernatant was transferred to a new microtube. Binding (70% alcohol was added), washing (the mixture was transferred to a tube containing the RNeasy column and centrifuged, then washed twice using RPE Buffer), and elution (RNA was eluted using RNA elution buffer, and centrifuged to remove RNA from the columns) were performed using a QIAcube (QIAGEN). RNA concentrations were determined using a NanoDrop 2000c Spectrophotometer (Thermo Scientific). Samples were diluted with RNase-free water for an RNA concentration of 500 ng/μL. cDNA synthesis from total RNA samples was carried out using the EasyScript™ cDNA Synthesis Kit (G236, Abm) and Rotor-Gene PCR (QIAGEN). RNA samples (1–2 μg) and primers (oligo(dT)) were heated at 65°C for 5 min and then cooled for 1 min. Subsequently, 5X EasyScript™ Reaction Buffer, dNTP Mix, RNase-free water, and EasyScript™ Reverse Transcriptase were added, and the final volume was adjusted to 20 μL, mixing thoroughly. This mixture was incubated at 42°C for 30–60 min using the Rotor-Gene PCR (QIAGEN, Hilden, Germany). At the end of the reaction, the mixture was heated at 70°C for 15 min to stop the enzyme activity. The resulting cDNA was stored at −20°C for a maximum of 2 months.

Quantitative RT-qPCR protocol for analyzing gene expression

The expression levels of genes related to pancreatic development and beta cell differentiation (*pdx1, ptf1, hnf1a, pax4*, and *nkx6.1*), insulin synthesis and secretion (*ins, slc2a*, and *kcnj11*), the circadian clock (*bmal1a, clock1a, per1b*, and *cry2a*), and oxidative stress (*fth1b, hmox1a, nqo1*, and *txnrd1*) were determined using β-actin gene sequences as a reference. The primers used for RT-PCR are listed in Table 1. BlasTaq 2X qPCR Master Mix (G891, Abm) was used for gene expression analysis. For each sample, 10 μL of BlasTaq 2X qPCR Master Mix, 0.6 μL of forward primer (300 nM), 0.6 μL of reverse primer (300 nM), and diluted cDNA were added to achieve a final volume of 20 μL. After thoroughly mixing the solution, the PCR tubes were subjected to 40 cycles of 2 min of preheating at 95°C, 15 s of denaturation at 95°C, 30 s of hybridization at 60°C, and 30 s of extension at 72°C. Three technical replicates were performed for each group. The relative expression of genes was analyzed and quantified using the comparative ΔΔCt method for each sample and the internal control (β-actin): ΔΔCt = 2^−(ΔCtsample − ΔCtinternal control).[25]

TABLE 1 Oligonucleotide primer sequences for quantitative real-time PCR.

Gene	Nucleotide sequences (Forward/Reverse)
Pancreas and beta cell Development-related genes	
pdx1	5'-TCACACGCACGCATGGAAAG-3'/ 5'-GCTCTGGTGTAAGCTGTGCG-3'
pax4	5'-ACAGAGAGAGCCTGCAGAGG-3'/ 5'-GCGGTTCTGCTTCGATGAGC-3'
hnf1a	5'-TCTGCAGTCCACTTCACCTG-3'/ 5'-CTCCACAGCTTTTGGAGGAG-3'
ptf1a	5'-GCAGTCGGACATGCCAATTC-3'/ 5'-GATCTTGTTCCTCGGTGGCA-3'
nkx6.1	5'-TTGTCTGGACTGCCCCGTTT-3'/ 5'-AGGGGTTTGGGATAGCGAGC-3'
Insulin synthesis and secretion genes	
slc2a2	5'-GCCGTTTGCTGGCACTTCAT-3'/ 5'-GCGTAGTGCCGCTCAATGAC-3'
ins	5'-GCTCTGTTGGTCCTGTTGGT-3'/ 5'-GGGCAGATTTAGGAGGAAGG-3'
kcnj11	5'-GTGCTTCATGTTTCGCCTTG-3'/ 5'-GGATGTCTATCTGGTCCAAAGG-3'
Circadian clock genes	
clock1a	5'-GACACCACCAGACCTCCACT-3'/ 5'-CCAGAATTCAGTGCAAGCAA-3'
bmal1a	5'-CCTGGACCAAAGAAGTGGAA-3' 5'-CATCACTTCCTCTGCGATCA-3'
per1b	5'-CCACAGGCTCCTAGTTCAGC-3'/ 5'-CCGTTTGTCTTGACCATGTG-3'
cry2a	5'-ACCAACAACTGTCCCGCTAC-3'/ 5'-CAACAGAGCCGCTTGATACA-3'
Oxidative stress response genes	
fth1b	5'-AATGTGAGGCGGCAATAAAC-3'/ 5'-CGTCCTCCTCTCTGGTTCTG-3'
hmox1a	5'-CCACGTCAGAGCTGAAAACA-3'/ 5'-CGAAGAAGTGCTCCAAGTCC-3'
nqo1	5'-CTCAAGGATTTGCCTTCAGC-3'/ 5'-CGCAGCACTCCATTCTGTAA-3'
txnrd1	5'-GGGAAGACTCTTGTGGTGGG-3, 5'-CTCGCAGCAGAATAGAGCGA-3'
β-Actin	5'-AAGCAGGAGTACGATGAGTCTG-3'/ 5'-GGTAAACGCTTCTGGAATGAC-3'

Biochemical methods

At 72 hpf, 30 embryos from each group were anesthetized with 0.02% MS-222 and homogenized in 300 μL of 0.9% NaCl solution using a homogenizer (Tissuelyser LT,

Qiagen) at 50 oscillations per second for 2 min. MDA levels were measured from the homogenate, while NO levels, SOD activity, and GSH levels were determined from the supernatant.

Total protein

The Lowry method was used to assess the total protein levels in the experimental groups.[31] After homogenization, supernatants were diluted with 0.9% NaCl at a 1:2 ratio. To 0.5 mL of the diluted supernatant, 3 mL of freshly prepared alkaline copper solution (containing 2 g $NaCO_3$, 0.4 g NaOH, 0.2 g copper sulfate, and 0.4 g sodium potassium tartrate) was added. Then, 0.1 mL of Folin reagent (which is reduced by Cu^{+2} ions in the alkaline protein solution) was added, followed by a 10-minute incubation at 25°C. Absorbance was measured at 500 nm using a spectrophotometer (Shimadzu UV-1280, Kyoto, Japan). Protein levels were calculated in mg/dL based on a standard curve prepared with 5, 10, and 15 mg/dL albumin standards. A 0.9% NaCl solution was used as the blank. Three technical replicates were performed for each group. The results for MDA, NO levels, and SOD activity were normalized to protein content.

Lipid peroxidation (LPO)

Malondialdehyde, a marker of LPO, was determined using thiobarbituric acid reactive substances according to the Yagi method.[32] To 0.25 mL of tissue homogenate, 1.25 mL of 1.22 M trichloroacetic acid in 0.6 M HCl and 0.75 mL of 0.047 M thiobarbituric acid were added and mixed, followed by incubation in a boiling water bath for 30 min. Then, 2 mL of n-butanol was added and the mixture was transferred to polyethylene tubes. After centrifugation at 3000 rpm for 10 min, the butanol phase was collected, and absorbance was measured at 532 nm. A 100% n-butanol solution was used as the blank. Three technical replicates were performed for each group. The results were expressed as nmol MDA/mg protein, using a molar extinction coefficient of $1.56 \times 10^5\ M^{-1}\,cm^{-1}$.

Nitric oxide (NO)

NO levels were measured using the Griess reagent.[33] Nitrite, reduced by vanadium chloride, forms a diazonium complex with sulfanilamide and N-(1-naphthyl) ethylenediamine dihydrochloride in an acidic environment. To 0.15 mL of supernatant, equal volumes of 0.15 mL 0.3 M NaOH and 0.15 mL 10% $ZnSO_4$ were added, followed by centrifugation at 14,000 rpm for 10 min. The deproteinized 0.1 mL samples were then treated with 0.1 mL of 1% VCl_3 solution, 0.05 mL of 2% sulfanilamide, and 0.05 mL of 0.1% N-(1-naphthyl)ethylenediamine dihydrochloride solutions, and incubated at 37°C for 30 min. Distilled water was used as the blank control. Each group was determined with three technical replicates. The absorbance of the diazonium complex was measured at 540 nm, and the results were expressed as nmol NO/mg protein.

Superoxide dismutase (SOD) activity

SOD activity was measured according to the Mylorie method.[34] Supernatants were diluted 1:40 in 0.9% NaCl solution. To 0.1 mL of diluted supernatant, 2.6 mL of 50 mM phosphate buffer (pH: 7.8), 0.1 mL of 6 mM o-dianisidine, and 0.2 mL of 0.2 mM riboflavin were sequentially added. For the blank tube, 0.1 mL of distilled water was used instead of the diluted supernatant. Absorbance at 460 nm was recorded as the baseline (0 min). The samples were then incubated for 8 min at room temperature inside a box illuminated by a 20-watt fluorescent lamp (420 nm), and absorbance was recorded again at 460 nm at 8 min. Distilled water was used as the blank control. Each group was determined with three technical replicates. The concentration was calculated based on the kinetic absorbance readings and expressed as U/min.mg protein.

Glutathione (GSH)

GSH levels were measured according to the Beutler method.[35] Supernatants were deproteinized with 2% metaphosphoric acid. 0.3 M Na2HPO4 and 40 mg/dL 5.5′-dithiobis 1–2 nitrobenzoic acid solution (Ellman's reagent) were added to the deproteinized fluid, respectively. Distilled water was used as the blank control. Each group was determined with three technical replicates. The absorbance of the colored product, resulting from the reaction of glutathione sulfhydryl groups with Ellman's reagent, was recorded at 412 nm. The results were expressed as mg/dL using a molar extinction coefficient of $13{,}600\ M^{-1}\,cm^{-1}$.

Evaluation of locomotor activities

The movement activity of zebrafish embryos was independently assessed at 72 hpf using a modified version of Foody's thigmotaxis response method.[36] During the experiment, the ambient temperature was maintained at a constant 28°C under a light/dark cycle of 14 h light and

10 h dark, using E3 solution. Embryos ($n = 15$ per group) were placed in the center of a 11 mm petri dish under constant light conditions (400 lux, 6200 K, fluorescent bulb), and allowed to acclimate for 30 s. The tail fin of each embryo was gently touched. The total observation time for each embryo was set to 15 s, and a camera (Canon EOS 20D) positioned 30 cm above (z-axis) recorded the embryos' movements. The camera was configured to shoot at a resolution of 1080p and a frame rate of 60 fps. Average speed (the distance covered by the embryo after the stimulus (touch) divided by the time (mm/s)), exploration rate (the percentage change in the rate at which the embryo explored or entered new areas after the stimulus (touch) between groups), and total distance traveled (the amount of distance the embryo moved in a given period following the stimulus (touch)) were analyzed using the pre-calibrated ToxTrac (open-source executable software) tracking software. Results were expressed as mean ± standard deviation. The internal control was the Cont group (3200 K, 400 lux) under a normal light cycle.

Statistical analysis

All statistical analyses were performed using GraphPad Prism 9.0 (GraphPad Software) to assess the effects of changes in pancreatic development, beta cell differentiation, insulin secretion-related genes, locomotor activity tests, and oxidative stress parameters in zebrafish embryos. The normality of the data was evaluated using the Shapiro–Wilk test, confirming that all parameters were normally distributed. One-way ANOVA was applied for comparisons among three or more groups, followed by Tukey's post-hoc test for multiple comparisons. Data are expressed as mean ± standard deviation (SD), with $p < 0.05$ considered the threshold for significance.

RESULTS

Gene expression results related with pancreatic development, beta cell development, and insulin secretion

When molecularly evaluating the differentiation of pancreatic cells into endocrine cells, the expression of *pdx1* and *hnf1a* significantly increased in both G (p_{pdx1}=0.0011, p_{hnf1a}=0.0016) and R (p_{pdx1}=0.0002, p_{hnf1a}<0.0001) groups compared to the Cont group. Additionally, the expressions of *pdx1* and hnf1a were significantly decreased in the G group compared to the R group (p_{pdx1}=0.0006, p_{hnf1a}=0.0016) (Figure 1A, Figure 1C). Furthermore, the upregulation of pax4 in beta cell differentiation (F_{ANOVA} (1.340, 2.679) = 1348, p_{ANOVA}= 0.0001) significantly decreased in both the Cont ($p < 0.0001$) and G ($p = 0.0002$) groups compared to the R group (Figure 1B, Table 2).

The role of *ptf1a* in pancreatic exocrine cell differentiation (F_{ANOVA}(1.007, 2.014) = 681.5, p_{ANOVA}= 0.0014) significantly increased in both G ($p = 0.0019$) and R ($p = 0.0016$) groups compared to the Cont group, while it significantly decreased in the R group compared to the G group (95% CI=(2.918–4.717), $p = 0.0022$, Figure 1D, Table 2).

The expressions of *nkx6.1* and *kcnj11* significantly increased in both G ($p_{nkx6.1}$= 0.0181, p_{kcnj11}=0.0016) and R ($p_{nkx6.1}$= 0.0106, p_{kcnj11}=0.0015) groups compared to the Cont group; there was also a significant increase in both gene expressions in the R group compared to the G group ($p_{nkx6.1}$= 0.0065, p_{kcnj11}=0.0009, Figure 1D, Figure 1E, Figure 1H, Table 2). The expressions of *slc2a2* and *ins* significantly increased in the G (pslc2a2<0.0001, pins<0.0001) and R (p_{slc2a2}=0.0013, p_{ins}=0.0003) groups compared to the Cont group. Similarly, there was a significant increase in both gene expressions in the R group compared to the G group (95% CI for *slc2a2*=(7.732–9.983), p_{slc2a2}=0.0022, 95% CI for *ins*=(16.69–20.90), p_{ins}<0.0001, Figure 1F, Figure 1G, Table 2).

Results of pancreatic and beta cell morphological assessment and comparison of insulin fluorescence signaling

Zebrafish embryos exposed to 0.5 watt 14/day monophasic G and R light conditions for 3 days. Pancreatic surface area measurements were performed using a Leica DMi8 inverted fluorescence microscope in the Tg(*ptf1a*:eGFP) jh1 line, and both beta cell area and insulin signals were assessed in the Tg(*ins*:mCherry)jh2 line. insulin fluorescence levels were expressed as CTCF. Compared to the Cont group, the pancreatic area increased by ~22.53% ($p = 0.0002$) in the G group and by ~97.13% ($p < 0.0001$) in the R group (Figure 2A,D). The pancreatic area in the G group was reduced by ~37.84% ($p < 0.0001$) when compared to the R group (Figure 2A,D). There were no significant differences in beta cell areas among all groups (p_{ANOVA} = 0.964, Figure 2B,D). The beta cell CTCF signal increased by ~50.27% ($p < 0.0001$) in the G group and by ~43.80% ($p < 0.0001$) in the R group compared to the Cont group. The beta cell CTCF signal was ~4.5% higher in the G group compared to the R group (F_{ANOVA} (1.898, 26.57) = 257.8, p_{ANOVA} <0.0001, 95%CI_{ins} = (127.6–5587), p_{Tukey} = 0.0398, Figure 2C,D).

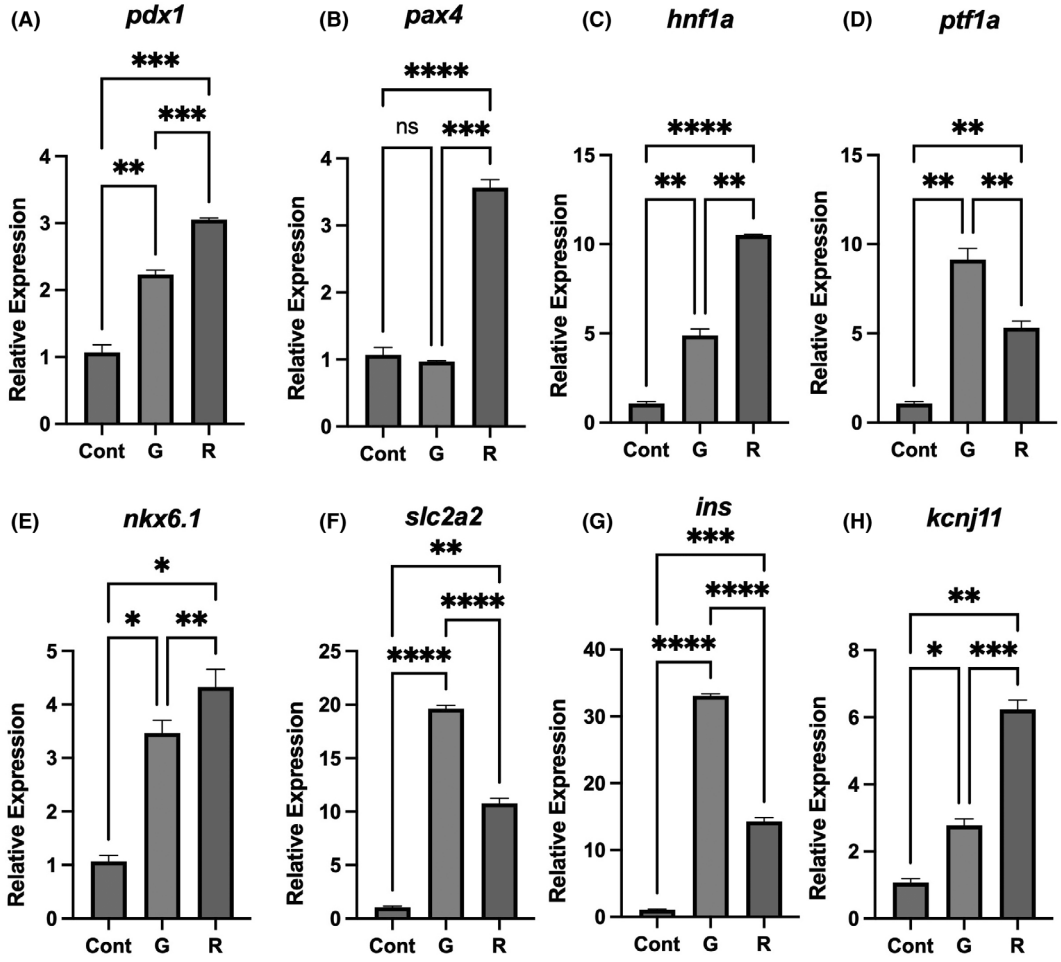

FIGURE 1 Expression levels of genes associated with pancreas and beta cell development in zebrafish embryos exposed to 0.5 watt 14/day monophasic G and R light conditions for 3 days. Expression of *pdx1* (A), *pax4* (B), *hnf1a* (C), *ptf1a* (D), *nkx6.1* (E), *slc2a2* (F), ins (G), and kcnj11 (H). Cont: control, G: green (520 nm) LED, R: red (660 nm) LED. Pools of 30 zebrafish embryos were created for each group, and experiments were performed with three technical replicates. Data are presented as mean ± SD. Statistical significance was assessed using ANOVA followed by Tukey post-hoc tests. ns: nonsignificantly different from another. *$p < 0.05$; **$p < 0.01$; ***$p < 0.001$; ****$p < 0.0001$, compared with each group.

Glucose level alterations in zebrafish embryos exposed to G (520 nm) and R (660 nm) LEDs

Glucose levels were assessed in whole-body homogenates of zebrafish embryos, with each group consisting of 30 embryos ($n = 30$ per group). Glucose levels significantly increased in both the G ($p = 0.0238$) and R groups (95% CI = −6.580 to −5.220, $p < 0.0001$) compared to the Cont group. Additionally, glucose levels in the G group were significantly lower compared to the R group ($p = 0.0045$, Figure 3).

Results of circadian cycle gene expression

The expression of clock1a and bmal1, positive regulators of the circadian cycle, significantly increased in the R group compared to the Cont group ($p_{clock1a}$ <0.0001, p_{bmal1} <0.0001, Figure 4A,B). The expression of bmal1 significantly decreased in the G group compared to the Cont group (95% CI = 0.1788–0.7908, p <0.0205, Figure 4B, Table 2).

Regarding the negative regulators of the cycle, per1b and cry2a expression significantly decreased in the G group compared to the Cont group ($p_{per1b} = 0.0057$, $p_{cry2a} = 0.0185$, Figure 4C, Figure 4D, Table 2). Additionally, *per1b* expression significantly increased in the R group, while *cry2a* expression significantly decreased compared to the Cont group (p_{per1b} <0.0001, $p_{cry2a} = 0.0212$, Figure 4C, Figure 4D, Table 2).

Results of oxidative stress gene expression

The presence of free iron ions in an oxidative stress environment contributes to the formation of ROS through Fenton-type reaction. Under hypoxic conditions caused by oxygen deficiency and oxidative stress, the expression of hmox1a

TABLE 2 Pancreatic, beta cell, insulin secretion, circadian clock, and oxidative stress gene expression levels, and quantitative PCR fold changes in zebrafish embryos exposed to 0.5 watt 14/day monophasic G and R light conditions for 3 days.

Gene symbol	Cont group expression Level	G (520 nm) expression level	R (660 nm) expression level	Fold change (G vs. Cont)	Fold change (R vs. Cont)	Fold change (G vs. R)	ANOVA *p*-value	*F*-value
Pancreas and beta cell development-related genes								
pdx1	1	2.23	3.05	2.23**	3.05***	−0.37***	$p=0.0001$	1240
pax4	1	0.97	3.56	−0.03	3.56****	−0.83***	$p=0.0001$	1348
hnf1a	1	4.9	10.51	4.9**	10.51****	−0.64***	$p=0.0004$	1997
ptf1a	1	9.14	5.32	9.14**	5.32**	1.72**	$p=0.0014$	681
nkx6.1	1	3.46	4.32	3.46*	4.32*	−0.20**	$p=0.0060$	164
Insulin synthesis and secretion genes								
slc2a2	1	19.63	10.77	19.63****	10.77****	1.82**	$p<0.0001$	2423
ins	1	33.08	14.28	33.08****	14.28***	2.31****	$p<0.0001$	4974
kcnj11	1	2.77	6.23	2.77*	6.23**	−0.66***	$p=0.0001$	537
Circadian clock genes								
clock1a	1	1.34	21.85	1.34	21.85****	−0.994****	$p<0.0001$	18,375
bmal1a	1	0.58	3.75	−0.42*	3.75****	−0.85****	$p<0.0001$	1767
per1b	1	0.37	8.88	−0.73**	8.88****	−0.96****	$p=0.0002$	2691
cry2a	1	2.24	0.43	2.24*	−0.67*	5.20*	$p=0.0093$	92
Oxidative stress genes								
fth1b	1	0.78	15.55	−0.22	15.55****	−0.95****	$p=0.0002$	2953
hmox1a	1	0.73	2.6	−0.21	2.6**	−0.72**	$p=0.0009$	322
nqo1	1	13.97	25.23	13.97***	25.23****	−0.45****	$p=0.0003$	3629
txnrd1	1	3.22	36.71	3.22****	36.71****	−0.92****	$p=0.0001$	6731

Note: Pools of 30 zebrafish embryos were created for each group, with experiments performed in three technical replicates. Data are presented as mean ± SD. The values in the table represent gene expression levels in the green and red groups normalized to the Cont group. The normalization was performed by setting the ΔΔCt value of the Cont group to 1, with the gene expression levels of the other groups scaled relative to this value. Statistical significance was assessed using ANOVA followed by Tukey post-hoc tests. Significant differences are denoted as follows: *$p<0.05$, **$p<0.01$, ***$p<0.001$, and ****$p<0.0001$.

Abbreviatons: Cont, control; G, green (520 nm) LED; R, red (660 nm) LED.

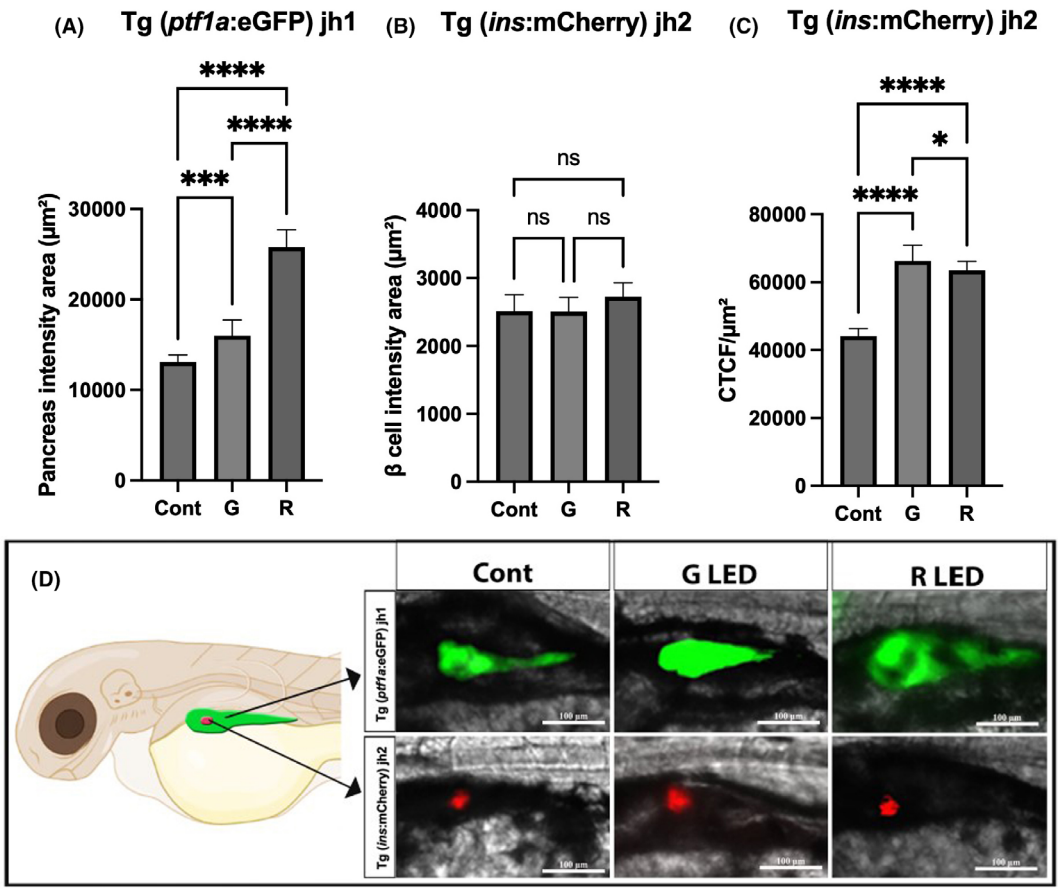

FIGURE 2 Measurement of pancreas, beta cell areas, and insulin fluorescence signaling in zebrafish at 72 hpf. Comparison of pancreatic area in Tg(*ptf1a*:EGFP) jh1 zebrafish (A). Comparison of total beta cell area in Tg(*ins*:MCherry)jh2 zebrafish (B). Comparison of corrected total cell fluorescence (CTCF) intensities of beta cells in Tg(*ins*:MCherry)jh2 zebrafish (C). Images of pancreas and beta cells in exposure groups (D). Cont: control, G: green (520 nm) LED, R: red (660 nm) LED. Data were shown as mean ± SD ($n = 15$ embryos). Statistical significance was assessed using ANOVA followed by Tukey post-hoc tests. *$p < 0.05$; **$p < 0.01$; ***$p < 0.001$; ****$p < 0.0001$. Scale bar: 100 µm.

increases, while *fth1b* serves as an antioxidant that binds to free iron ions. In the R group, the expressions of *fth1b* and *hmox1a* were significantly increased compared to the Cont group ($p_{fth1b} < 0.0001$, phmox1a = 0.0012) and the G group (p*fth1b* < 0.0001, p*hmox1a* = 0.0019) (Figure 5A, Figure 5B, Table 2). The expressions of *nqo1* and txnrd1 were also significantly increased in both the G ($p_{nqo1} = 0.0007$, $p_{txnrd1} < 0.0001$) and R ($p_{nqo1} < 0.0001$, $p_{txnrd1} < 0.0001$) groups compared to the Cont group (Figure 5C, Figure 5D, Table 2). When compared to the G group, the expression of nqo1 was significantly increased in the R group (95% CI = −12.27 to −10.26, $p < 0.0001$) (Figure 5C, Table 2).

Biochemical assessment of oxidative stress

The assessment of oxidative stress in PMD applications indicates how cells and tissues are affected by light. In our study, the levels of MDA, a product of lipid peroxidation, were significantly increased in the R group compared to both the Cont group ($p < 0.0001$) and the G group ($p = 0.0005$) (Figure 6A). NO levels significantly increased in the G group compared to the Cont group ($p = 0.0173$) and the R group (95% CI = 0.2149–0.9251, $p = 0.02$) (Figure 6B). SOD activities and GSH levels were significantly decreased in the G ($p_{SOD} = 0.0009$, $p_{GSH} < 0.0001$) and R ($p_{SOD} = 0.0039$, $p_{GSH} < 0.0001$) groups compared to the Cont group. In the R group, SOD and GSH levels were significantly increased compared to the G group ($p_{SOD} < 0.0001$, $p_{GSH} = 0.0074$) (Figure 6C,D).

Results of locomotor activity

In zebrafish embryos exposed to 0.5 watt, 14/24 h G and R light conditions at 72 h post-fertilization (hpf), the average speed, exploration rate, and total distance traveled were assessed after placing the embryos in the center of 11 cm petri dishes and applying a stimulus (touching the tail fin). The average speed was calculated as the distance traveled

(mm) divided by the time elapsed (s) after stimulation. The exploration rate was determined as the percentage change in the speed of exploring or entering new areas post-stimulation across the groups. The total distance traveled was defined as how far the embryo moved within a specified duration after the stimulus. These parameters were quantified using ToxTrac (open-source executable software).

Average speed significantly increased in the G group compared to the Cont group (95% CI = −15.25 to −2.47, $p = 0.0061$), while it significantly decreased in the R group (95% CI = 0.2521 to 13.59, $p = 0.0412$, Figure 7A). The exploration rate was significantly higher in both the G and R groups compared to the Cont group ($p < 0.0001$ for both groups, Figure 7B). The distance traveled in both exposure groups was significantly reduced compared to the Cont group ($p < 0.0001$ for both groups, Figure 7B, Figure 7C).

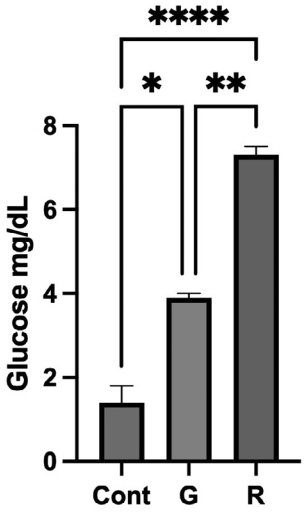

FIGURE 3 The effects of 0.5 watt 14/day G and R light conditions on glucose levels in zebrafish embryos at 72 hpf. Data are presented as mean ± SD obtained from three replicates per group (30 embryos per pool). Statistical significance was assessed using ANOVA followed by Tukey post-hoc tests. Significant differences are denoted as follows: *$p < 0.05$, **$p < 0.01$, ***$p < 0.001$, and ****$p < 0.0001$, Cont: control, G: green (520 nm) LED, R: red (660 nm) LED.

DISCUSSION

In this study, both the G and R groups promoted the morphological development of pancreatic exocrine and endocrine structures compared to the Cont group. Although there was an increase in the expression of genes supporting beta cell differentiation in the R group, the increase in beta cell insulin signaling was lower than that in the G group. The increase in *slc2a2* and ins expression levels in the G group, along with the ~2.25-fold increase in kcnj11 expression in the R group compared to the G group, supports this decrease in insulin signaling. The underlying mechanism for the reduced ins expression in the R group indicates a disrupted circadian rhythm and increased oxidative stress.

There are limited direct studies on the effects of G (520 nm) and R (660 nm) treatments on beta cells, although some research indicates that these wavelengths

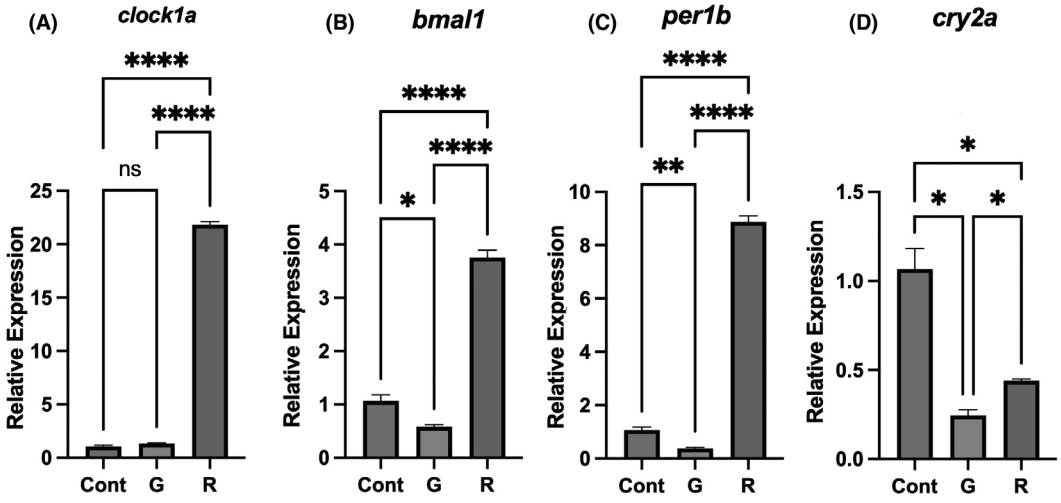

FIGURE 4 Expression of circadian cycle genes in zebrafish embryos exposed to 0,5 watt 14/per day monophasic G and R light conditions at 72 hpf. Expressions of *clock1a* (A), *bmal1*(B), *per1b*(C), *cry2a*(D). G: green (520 nm) LED, R: red (660 nm) LED. Pools of 30 zebrafish embryos were created for each group, and experiments were performed with three technical replicates. Data were shown as mean ± SD. Statistical significance was assessed using ANOVA followed by Tukey post-hoc tests. ns: nonsignificantly different from another. *$p < 0.05$; **$p < 0.01$; ***$p < 0.001$; ****$p < 0.0001$, compared with each group.

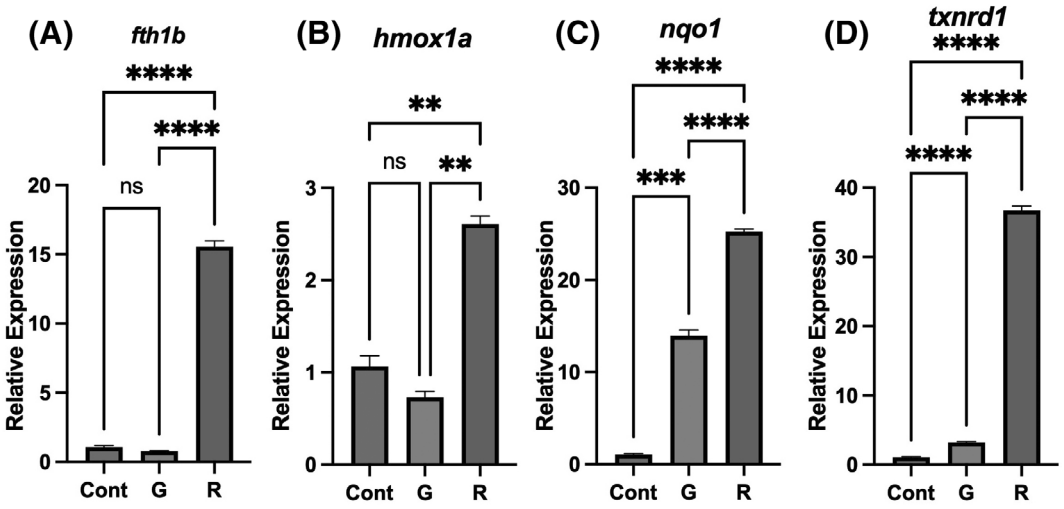

FIGURE 5 Expression of oxidative stress genes in zebrafish embryos exposed to 0,5 watt 14/per day monofazik G and R light conditions at 72 hpf. Expression of fth1a (A), hmox1a (B), nqo1(C), txnrd1 (D). Cont: control, G: green (520 nm) LED, R: red (660 nm) LED. Pools of 30 zebrafish embryos were created for each group, and experiments were performed with three technical replicates. Data were shown as mean ± SD. Statistical significance was assessed using ANOVA followed by Tukey post-hoc tests. ns: nonsignificantly different from another. *$p < 0.05$; **$p < 0.01$; ***$p < 0.001$; ****$p < 0.0001$, compared with each group.

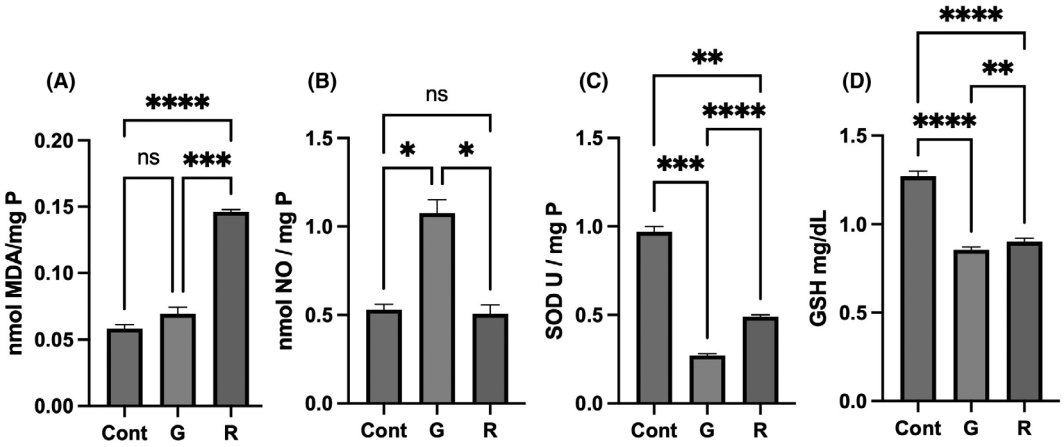

FIGURE 6 Biochemical analysis of oxidative stress in zebrafish embryos exposed to 0.5 watt monophasic 14 h/ day G (520 nm) and R (660 nm) light conditions at 72 hpf. Malondialdehide (MDA) (A); nitric oxide (NO) (B); superoxide dismutase (SOD) activities (C); glutathione (GSH) levels of groups (D). Cont: control, G: green (520 nm) LED, R: red (660 nm) LED. Pools of 30 zebrafish embryos were created for each group, and experiments were performed with three technical replicates. Data were shown as mean ± SD. Statistical significance was assessed using ANOVA followed by Tukey post-hoc tests. ns: nonsignificantly different from another. *$p < 0.05$; **$p < 0.01$; ***$p < 0.001$; ****$p < 0.0001$, compared with each group.

affect systemic effects and cellular activities. Growth hormone and insulin-like growth factor (IGF) support insulin secretion by regulating insulin production and calcium levels, thereby aiding growth, development, and regeneration.[37–39] It has been reported that G (520–550 nm) increases proliferation and 3D migration in human umbilical vein endothelial cells compared to R (620–660 nm),[40] and that it elevates IGF levels in Paralichthys olivaceus[41] and Takifugu rubripes fish,[42] supporting morphological growth. The increase in plasma IGF expression and insulin levels in juvenile barfin flounder following G (520 nm) treatment further supports this hypothesis.[2] Furthermore, G (530 nm) treatment has been shown to lead to an increase in the expression of the anti-apoptotic gene bcl-2 and promote morphological growth in juvenile Takifugu rubripes fish.[42] In zebrafish embryos, R (660 nm) treatment was reported to cause oxidative stress, resulting in an increase in apoptotic cell counts and higher mortality rates.[5] Similarly, our results indicate that G treatment leads to an increase in pancreatic area in zebrafish embryos compared to the R treatment group

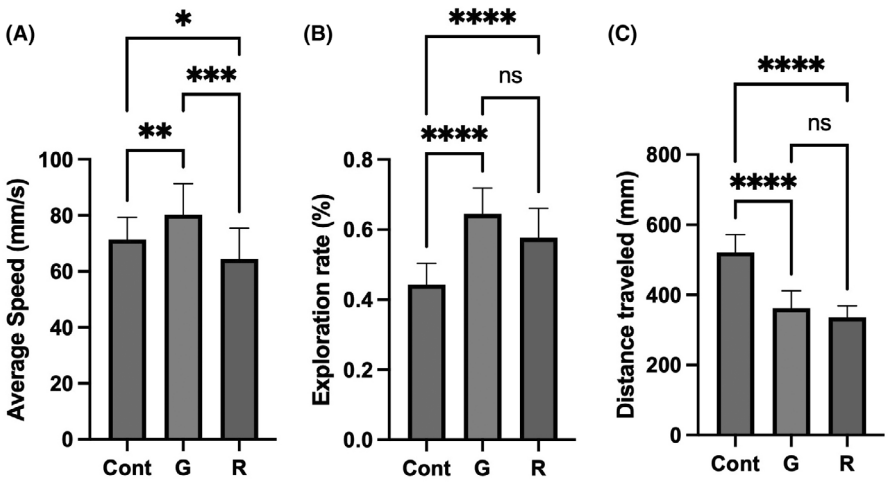

FIGURE 7 Locomotor activities of in zebrafish embryos exposed to 0.5 watt monophasic G (520 nm) and R (660 nm) light conditions at 72 hpf. Average speeds (A) of the groups, Exploration rate(B), Distance traveled (C). Cont: control, G: green (520 nm) LED, R: red (660 nm) LED. The locomotor activity test was performed on $n = 15$ embryos representing each group. The data are presented as mean ± SD. Statistical significance was evaluated using ANOVA followed by Tukey's post-hoc tests. ns: nonsignificantly different from other groups. *$p < 0.05$; **$p < 0.01$; ***$p < 0.001$; ****$p < 0.0001$, when compared between groups.

(p = <0.0001, Figure 2A). Although no significant difference was found in beta cell areas ($p_{ANOVA} = 0.964$, Figure 2B), there was a significant increase in insulin signaling in both G and R groups ($p < 0.0001$, Figure 2C). Additionally, the dramatically increase in *slc2a2* and *ins* expressions in the G group ($p_{slc2a2} < 0.0001$, $p_{ins} < 0.0001$, Figure 1F, Figure 1G) supports the increase in insulin signaling ($p < 0.05$). However, systemic R treatment led to an increase in gene expressions (pdx1, pax4, hnf1a, and nkx6.1) that support the differentiation of pancreatic progenitor cells into beta cells (Figure 1, Table 2). Similarly, Min SH et al. demonstrated that 4 weeks of local two-dimensional illuminated R (630/850 nm) treatment in adult rats provided protection in pancreatic islets, resulting in reduced hyperglycemia and increased serum insulin levels.[43] These results suggest that the systemic and local effects of R treatment are different. The evaluation of the stress effect exerted by R treatment on the central nervous system in systemic activities is beyond the scope of our study. However, the increase in neuropeptide Y levels, a neurohormone, that suppresses insulin secretion in juvenile red spotted (*Epinephelus akaara*) fish under R (590 nm) treatment for 2 months (12 h/day) indicates that insulin secretion is regulated by multiple factors.[44] Furthermore, in this study, we showed for the first time that 14 h/day R treatment for 3 days leads to an increase in the expression of the *kcnj11* ($p < 0.001$), which encodes the K-ATP channel subunit Kir6.2 and causes a decrease in *ins* expression ($p < 0.0001$) and insulin signaling ($p < 0.05$) compared to G treatment group (Figure 1G,H, Figure 2C, Table 2). Wang et al. demonstrated that G (540 nm) causes an increase in intracellular calcium levels in adipocyte cells differentiating into osteoblasts.[7] Previous studies and our findings indicate that G treatment promotes beta cell differentiation, enhancing insulin secretion through modulation of K-ATP channels and Ca ion channels. Despite methodological differences, the findings indicate that both G and R treatments increase insulin levels in peripheral tissues and promote glucose uptake, which may provide clinical benefits in metabolic syndrome, diabetes, and regulation of cellular metabolism.

There is a strong interaction between BMAL1 and CLOCK1A and antioxidant hormone melatonin secreted by the pineal gland.[8,24,45] Conditional transcriptional ablation of CLOCK and BMAL1 in pancreatic islets of mice leads to impaired beta cell function.[24] Increased melatonin secretion during the scotophase inhibits insulin secretion.[26] The desynchronization of melatonin and insulin contributes to metabolic syndrome and diabetes.[46] In our previous study, we demonstrated that 1 watt R treatment caused a decrease in melatonin (*aanat2*) expression in zebrafish.[8] While R treatment increases melatonin levels in *Amphiprion clarkii*,[47] G treatment increases melatonin levels in zebrafish embryos.[5] According to our findings, R treatment during the photophase increased the expression of the positive regulators of the circadian rhythm, *clock* and *bmal1*, compared to both the Cont and G treatments groups ($p < 0.0001$). In contrast, R treatment during the photophase resulted in an increase in the expression of the negative regulator of circadian rhythm, *per1b* ($p < 0.0001$), while *cry2a* expression decreased ($p < 0.05$). This indicates a disruption of the central controller of metabolic processes, the circadian rhythm. In light of these findings,

the reduction in *ins* expression and insülin signaling in the R group compared to the G group may be attributed to the disrupted circadian cycle and decreased melatonin levels. Melatonin neutralizes mitochondrial-derived free radicals in cells, reducing oxidative stress and improving mitochondrial function, thereby optimizing cellular energy production.[27] G (530 nm) treatment has been shown to prevent oxidative stress by reducing the levels of H_2O_2, a source of hydroxyl radicals (·OH), in species such as *Amphiprion clarkii*,[47] *Carassius auratus*,[48] and *Seriola lalandi*.[49] In our earlier study, we observed that 1 watt of G (520 nm) led to an increase in MDA levels against decreasing melatonin levels.[8] Similarly, Wang et al.[50] demonstrated that G (540 nm) light caused an increase in ROS levels in adipose-derived stem cells compared to R (660 nm) treatment. In this study, 0.5 watt/m^2 R LED treatment caused an increase in MDA levels compared to both the Cont ($p < 0.0001$) and G ($p < 0.001$) groups (Figure 2A). There was no significant difference between the G group and the Cont ($p = 0.12$). The reason for the contradiction between previous studies and our findings suggests that R treatment has a greater capacity to increase oxidative stress compared to G treatment, depending on the applied power and duration. Increased lipid peroxidation in R treatment compared to G treatment may cause an increase in fth1b, hmox1a, nqo1, txnrd1, a decrease in GSH, disruption of circadian cycles, and affecting insulin expression and secretion. R treatment supports cellular energy production by enhancing mitochondrial activity,[50] but in the long term, it can lead to excessive oxidative stress and inflammation, resulting in DNA damage, cellular aging, and the development of chronic diseases. The protective effects of G treatment in reducing oxidative stress and optimizing cellular energy production present promising potential for the treatment of metabolic diseases and diseases related to cellular damage.

The regulation of circadian rhythm and the balance of NAD/NADH redox by BMAL1 enhance the resistance of cells to oxidative damage.[51] The increased intracellular levels of NADH and NADPH through glycolysis and the pentose phosphate pathway have been reported to augment the binding of the CLOCK:BMAL1 complex to DNA.[51] This mechanism facilitates the maintenance of the photophase period, which has high energy demands. Moreover, elevated NADPH levels help preserve the levels of reduced glutathione (GSH), a potent antioxidant.[52] Inhibition of the pentose phosphate pathway, which is the primary source of NADPH,[53] can extend the circadian period of clock gene expression in cells. In our study, R treatment resulted in lipid peroxidation and increased MDA levels. The decrease in GSH levels observed in the R group in response to increased damage may also be attributed to reduced NADPH levels due to pentose phosphate pathway inhibition. Pir R. et al. explained that R treatment significantly lowered the light/dark ratio (indicating wakefulness and activity measurement) in zebrafish embryos.[5] Furthermore, R treatment increases the activation of cytochrome C (COX, also known as Complex IV), facilitating the reduction of oxygen to water and generating the proton gradient necessary for ATP synthase, thereby enhancing ATP production.[20,50] Wang et al. found that a 3 h R (660 nm) treatment increases ATP levels in adipocyte-derived stem cells compared to G (540 nm) treatment, suggesting that G treatment is safer.[50] The COX-dependent increase in ATP induced by R treatment explains the enhanced energy (ATP)-dependent motility observed in adult zebrafish, tilapia, and ram sperm cells.[54,55] Conversely, uncontrolled increases in COX activity can lead to increased oxygen consumption in cells. When sufficient oxygen is not available, cells may enter a hypoxic state, contributing to oxidative stress. During excessive COX activity, electron leakage can result in the formation of partially reduced oxygen species that can damage cellular components such as DNA, proteins, and lipids.[5,56] In this study, the increased MDA levels in the R group compared to the control group ($p < 0.0001$, Figure 2A), along with elevated glucose levels in the R group ($p < 0.0001$, Figure 3), indicate a disruption in cellular energy balance due to oxidative stress. Given that the disrupted energy balance under hypoxic conditions may lead to neuroinflammation and cognitive dysfunction in the central nervous system,[57] the increased oxidative stress in the R group explains the reduction in average speed compared to the control group (95% CI = 0.2521–13.59, $p = 0.0412$, Figure 7A). In contrast, there was a significant increase in average speed in the G group compared to both the control ($p < 0.001$) and R groups ($p < 0.0001$) (Figure 7A). Similarly, Pir R. et al. reported that compared to the GLED group, zebrafish in the RLED group exhibited increased expression levels of 8-hydroxy-2′-deoxyguanosine (8-OHdG), a marker of mitochondrial DNA damage, along with elevated levels of Hsp70, as well as decreases in activity, heart rate, and blood flow.[5] Under high oxygen concentrations, COX predominantly exists in an oxidized state, consuming NO. When COX is significantly reduced, NO is not consumed and accumulates in the microenvironment, which has implications for both cellular respiration rates and local vascular tone.[58] The increased NO levels observed with GLED treatment ($p < 0.05$, Figure 6B) suggest that electron flow in the electron transport chain remains intact and that increased blood flow and oxygen uptake in the pancreas may enhance insulin expression. These findings indicate that G treatment has positive effects on cellular energy balance, oxidative stress, and mitochondrial functions in zebrafish, ultimately enhancing motor functions.

The current study has several limitations. First, while zebrafish provide a significant advantage in evaluating the

systemic effects of light, the applicability of the results to other mammalian models or human physiology may be limited. Second, the wavelength, power, light permeability, and application method (local or systemic) of light used in PBM therapy are important factors. Third, this study evaluated treatments in the wavelength range of 510–540 nm for green LED and 620–660 nm for red LED. Therefore, the dosage and exposure time of the LED lights used in our study may not be optimized for different organisms or tissues, which restricts the generalizability of the results. Finally, while our focus on systemic effects rather than local effects demonstrates the advantages of using zebrafish as a model organism in such holistic analyses, it should also be noted that specific wavelengths in specific cell types require more detailed investigation of local responses.

G treatment contributes to the enhancement of insulin expression, beta cell differentiation, and function. These results hold promise for the treatment of diabetes, metabolic syndrome, and pancreatic diseases. This study represents the first investigation focused on pancreatic development and beta cell functions. The effects of cellular energy metabolism, particularly on beta cell development and functionality, should be considered in light of the varying wavelengths, dosages, and exposure times of LED light sources. Therefore, further studies are needed to elucidate the mechanisms underlying beta cell differentiation associated with different light spectra.

In conclusion, our study elucidates the effects of green and red LED lights on pancreatic development, beta cell differentiation, insulin signaling, and circadian rhythms. G treatment may be more effective in promoting pancreatic development and insulin signaling compared to R. Conversely, while R promotes the differentiation of pancreatic progenitor cells into beta cells, it may also lead to a reduction in insulin signaling associated with increased oxidative stress and disrupted circadian rhythms. These findings provide a new perspective on understanding the effects of light-based therapeutic approaches on pancreatic development and metabolic processes, suggesting that different LED wavelengths could serve as potential tools in the treatment of cellular metabolic disorders.

AUTHOR CONTRIBUTIONS

The authors declare that all data were generated in-house and that no paper mill was used. All authors contributed to the study's conception and design. The study was designed and supervised by Prof. Dr. Ebru Emekli-Alturfan. Material preparation and data collection were performed by Ünsal Veli Üstündağ, İsmail Ünal, Derya Cansız, Merih Beler, Naveen Krishna Kanagaraj, Amrish Rajendra Kumar. The manuscript was written by Ünsal Veli Üstündağ in consultation with Dr. Ravindra Peravali and Prof. Dr. Ebru Emekli-Alturfan. All authors read and approved the final manuscript.

ACKNOWLEDGMENTS

This project has been supported by the Scientific and Technological Research Council of Türkiye (TÜBİTAK) 2214A Program and Scientific Research Projects Foundation (BAP) of the Marmara University of [Project No: TDK-2021-10172]. This study was produced from PhD thesis of Ünsal Veli Üstündağ.

CONFLICT OF INTEREST STATEMENT

All of the authors do not have financial interests or personal relationships to disclose.

ETHICS STATEMENT

No ethical approval was required for the techniques utilized because the zebrafish embryos used were no older than 5 days old, as indicated by the Council of Europe (1986), Directive 86/609/EEC.

ORCID

Ünsal Veli Üstündağ https://orcid.org/0000-0003-0804-1475
İsmail Ünal https://orcid.org/0000-0002-8664-3298
Derya Cansız https://orcid.org/0000-0002-6274-801X
Merih Beler https://orcid.org/0000-0002-6408-5571
Naveen Krishna Kanagaraj https://orcid.org/0009-0009-5669-9336
Amrish Rajendra Kumar https://orcid.org/0009-0007-2521-8750
Ravindra Peravali https://orcid.org/0000-0002-8168-5392
Ebru Emekli-Alturfan https://orcid.org/0000-0003-2419-8587

REFERENCES

1. Yeh N, Ding TJ, Yeh P. Light-emitting diodes' light qualities and their corresponding scientific applications. *Renew Sustain Energy Rev*. 2015;51:55-61.
2. Takahashi A, Kasagi S, Murakami N, et al. Chronic effects of light irradiated from LED on the growth performance and endocrine properties of barfin flounder *Verasper moseri*. *Gen Comp Endocrinol*. 2016;232:101-108.
3. Kwon J, Kim SH, Park DH. Duodenal multi-wavelength photobiomodulation with light-emitting diode improves glycemic control and hepatic parameters in type 2 diabetes animal model. *Mech Photobiomodul Therapy XVII*. 2023;12362:29-32.
4. Castro KMR, de Paiva Carvalho RL, Junior GMR, et al. Can photobiomodulation therapy (PBMT) control blood glucose levels and alter muscle glycogen synthesis? *J Photochem Photobiol B*. 2020;207:111877.
5. Pir R, Sulukan E, Şenol O, et al. Co-exposure effect of different colour of LED lights and increasing temperature on zebrafish larvae

(Danio rerio): Immunohistochemical, metabolomics, molecular and behaviour approaches. *Sci Total Environ*. 2024;951:175468.
6. Yuan SS, Xu HZ, Liu LQ, Zheng JL. Different effects of blue and red light-emitting diodes on antioxidant responses in the liver and ovary of zebrafish Danio rerio. *Fish Physiol Biochem*. 2017;43:411-419.
7. Wang Y, Huang YY, Wang Y, Lyu P, Hamblin MR. Photobiomodulation (blue and green light) encourages osteoblastic-differentiation of human adipose-derived stem cells: role of intracellular calcium and light-gated ion channels. *Sci Rep*. 2016;6(1):33719.
8. Üstündağ ÜV, Çalıskan-Ak E, Ateş PS, et al. White LED light exposure ınhibits the development and xanthophore pigmentation of zebrafish embryo. *Sci Rep*. 2019;9(1):1-12.
9. Dauchy RT, Wren MA, Dauchy EM, et al. The influence of red light exposure at night on circadian metabolism and physiology in Sprague-Dawley rats. *J Am Assoc Lab Anim Sci*. 2015;54(1):40-50.
10. Ayuk SM, Houreld NN, Abrahamse H. Effect of 660 nm visible red light on cell proliferation and viability in diabetic models in vitro under stressed conditions. *Lasers Med Sci*. 2018;33:1085-1093.
11. Gupte JM, Spaeth M, Perelis M, et al. Defining a novel role for the Pdx1 transcription factor in islet β-cell maturation and proliferation during weaning. *Diabetes*. 2017;66:2830-2839.
12. Heller S, Melzer MK, Azoitei N, Julier C, Kleger A. Human pluripotent stem cells go diabetic: a glimpse on monogenic variants. *Front Endocrinol (Lausanne)*. 2021;12:468284.
13. Gage BK, Baker RK, Kieffer TJ. Overexpression of PAX4 reduces glucagon expression in differentiating hESCs. *Islets*. 2014;6:e29236.
14. Duque M, Amorim JP, Bessa J. Ptf1a function and transcriptional cis-regulation, a cornerstone in vertebrate pancreas development. *FEBS J*. 2022;289(17):5121-5136.
15. Memon B, Abdelalim EM. Stem cell therapy for diabetes: beta cells versus pancreatic progenitors. *Cells*. 2020;9(2):283.
16. Fu Z, Gilbert ER, Liu D. Regulation of insulin synthesis and secretion and pancreatic Beta-cell dysfunction in diabetes. *Curr Diabetes Rev*. 2013;9:25-53.
17. Rutter GA, Pullen TJ, Hodson DJ, Martinez-Sanchez A. Pancreatic β-cell identity, glucose sensing and the control of insulin secretion. *Biochem J*. 2015;466:203-218.
18. He L, He T, Farrar S, Ji L, Liu T, Ma X. Antioxidants maintain cellular redox homeostasis by elimination of reactive oxygen species. *Cell Physiol Biochem*. 2017;44(2):532-553.
19. Girard CA, Shimomura K, Proks P, et al. Functional analysis of six Kir6. 2 (KCNJ11) mutations causing neonatal diabetes. *Pflugers Arch*. 2006;453(3):323-332.
20. Ferraresi C, Parizotto NA, Pires de Sousa MV, et al. Light-emitting diode therapy in exercise-trained mice increases muscle performance, cytochrome c oxidase activity, ATP and cell proliferation. *J Biophotonics*. 2015;8(9):740-754.
21. Cao X, Yang Y, Selby CP, Liu Z, Sancar A. Molecular mechanism of the repressive phase of the mammalian circadian clock. *Proc Natl Acad Sci*. 2021;118(2):e2021174118.
22. Chan K, Wong FS, Pearson JA. Circadian rhythms and pancreas physiology: a review. *Front Endocrinol*. 2022;13:920261.
23. Sadacca LA, Lamia KA, Delemos AS, Blum B, Weitz CJ. An intrinsic circadian clock of the pancreas is required for normal insulin release and glucose homeostasis in mice. *Diabetologia*. 2011;54:120-124.
24. Marcheva B, Ramsey KM, Buhr ED, et al. Disruption of the CLOCK components CLOCK and BMAL1 leads to hypoinsulinaemia and diabetes. *Nature*. 2010;466(7306):627-631.
25. Seshadri N, Doucette CA. Circadian regulation of the pancreatic beta cell. *Endocrinology*. 2021;162(9):bqab089.
26. Peschke E, Bähr I, Mühlbauer E. Melatonin and pancreatic islets: interrelationships between melatonin, insulin and glucagon. *Int J Mol Sci*. 2013;14(4):6981-7015.
27. Sener G, Sehirli AÖ, Keyer-Uysal M, Arbak S, Ersoy Y, Yeğen BÇ. The protective effect of melatonin on renal ischemia–reperfusion injury in the rat. *J Pineal Res*. 2002;32(2):120-126.
28. Whitmore D, Foulkes NS, Sassone-Corsi P. Light acts directly on organs and cells in culture to set the vertebrate circadian clock. *NATNEWS*. 2000;404:87-91.
29. European Commission. Council directive 86/609/EEC of 24 November 1986 on the approximation of laws, regulations and administrative provisions of the member states regarding the protection of animals used for experimental and other scientific purposes. *Off J Eur Union*. 1986;358:1-28.
30. Westerfield M. *The Zebrafish Book; A Guide for the Laboratory Use of Zebrafish (Danio Rerio)*. Eugene, Oregon USA: University of Oregon Press; 2007
31. Lowry OH, Rosebrough NJ, Farr AL, Randall RJ. Protein measurement with the Folin phenol reagent. *J Biol Chem*. 1951;193(1):265-275.
32. Yagi K. Assay for blood plasma or serum. *Methods Enzymol*. 1984;105:328-331.
33. Miranda KM, Espey MG, Wink DA. A rapid, simple spectrophotometric method for simultaneous detection of nitrate and nitrite. *Nitric Oxide*. 2001;5(1):62-71.
34. Mylroie AA, Collins H, Umbles C, Kyle J. Erythrocyte superoxide dismutase activity and other parameters of copper status in rats ingesting lead acetate. *Toxicol Appl Pharmacol*. 1986;15:512-520.
35. Beutler E. *Gluthatione: Red Cell Metabolism A Manual Biochemical Methods*. Grune and Stratton; 1975.
36. Goody MF, Kelly MW, Reynolds CJ, Khalil A, Crawford BD, Henry CA. NAD+ biosynthesis ameliorates a zebrafish model of muscular dystrophy. *PLoS Biol*. 2012;10(10):e1001409.
37. Holt RIG, Simpson HL, Sönksen PH. The role of the growth hormone–insulin-like growth factor axis in glucose homeostasis. *Diabet Med*. 2003;20(1):3-15.
38. Gauthier BR, Wollheim CB. Synaptotagmins bind calcium to release insulin. *J Pineal Res*. 2008;295(6):E1279-E1286.
39. Lin CH, Hwang PP. The control of calcium metabolism in zebrafish (Danio rerio). *Int J Mol Sci*. 2016;17(11):1783.
40. Rohringer S, Holnthoner W, Chaudary S, et al. The impact of wavelengths of LED light-therapy on endothelial cells. *Sci Rep*. 2017;7(1):1-11.
41. Zou Y, Peng Z, Wang W, et al. The stimulation effects of green light on the growth, testicular development and stress of olive flounder Paralichthys olivaceus. *Aquaculture*. 2022;546:737275.
42. Liu S, Fang Y, Liu Y, et al. Effects of different LED spectra on growth and expression of GH/IGF-I axis and apoptosis related genes in juvenile Takifugu rubripes. *Front Mar Sci*. 2022;9:1008068.
43. Min SH, Kwon J, Do EJ, et al. Duodenal dual-wavelength photobiomodulation improves hyperglycemia and hepatic parameters with alteration of gut microbiome in type 2 diabetes animal model. *Cell J*. 2022;11(21):3490.

44. Xu W, Zou H, Zeng J, Mei W, Choi S. Effects of various LED light spectra on growth, gonadal development, and growth−/reproduction-related hormones in the juvenile red spotted grouper, *Epinephelus akaara*. *Animals*. 2023;13(13):2047.
45. Sacksteder RE, Kimmey JM. Immunity, infection, and the zebrafish clock. *Infect Immun*. 2022;90(9):e0058821.
46. Robeva R, Kirilov G, Tomova A, Kumanov P. Melatonin–insulin interactions in patients with metabolic syndrome. *J Pineal Res*. 2008;44(1):52-56.
47. Choi CY, Shin HS, Lee J, Kil GS. Effects of retinal light input on circadian rhythm genes in the yellowtail clownfish (Amphiprion clarkii) as determined using LED light spectra. *Biol Rhythm Res*. 2014;45(5):671-683.
48. Jung SJ, Choi YJ, Kim NN, Choi JY, Kim BS, Choi CY. Effects of melatonin injection or green-wavelength LED light on the antioxidant system in goldfish (*Carassius auratus*) during thermal stress. *Fish Shellfish Immunol*. 2016;52:157-166.
49. Choi YJ, Choi JY, Yang SG, Kim BS, Choi CY. The effect of green and red light spectra and their intensity on the oxidative stress and non-specific immune responses in gold-striped amberjack. *Seriola Lalandi Mar Freshw Behav Phy*. 2016;49(4):223-234.
50. Wang Y, Huang YY, Wang Y, Lyu P, Hamblin MR. Red (660 nm) or near-infrared (810 nm) photobiomodulation stimulates, while blue (415 nm), green (540 nm) light inhibits proliferation in human adipose-derived stem cells. *Sci Rep*. 2017;7(1):7781.
51. Sato F, Kohsaka A, Bhawal UK, Muragaki Y. Potential roles of Dec and Bmal1 genes in interconnecting circadian clock and energy metabolism. *Int J Mol Sci*. 2018;19(3):781.
52. Bradshaw PC. Cytoplasmic and mitochondrial NADPH-coupled redox systems in the regulation of aging. *Nutrients*. 2019;11(3):504.
53. Rey G, Valekunja UK, Feeney KA, et al. The pentose phosphate pathway regulates the circadian clock. *Cell Metab*. 2016;24(3):462-473.
54. You MS, Yang WB, Cheng CH, Yu S, Chang HC, Yu HS. Red LED light treatment promotes cognitive learning through upregulation of trpm4 in zebrafish. *J Photochem Photobiol B Biol*. 2020;213:112073.
55. Zan-Bar T, Bartoov B, Segal R, et al. Influence of visible light and ultraviolet irradiation on motility and fertility of mammalian and fish sperm. *Photomed Laser Surg*. 2005;23(6):549-555.
56. Blanco-Prieto O, Catalán J, Trujillo-Rojas L, et al. Red LED light acts on the mitochondrial electron chain of mammalian sperm via light-time exposure-dependent mechanisms. *Cells*. 2020;9(12):2546.
57. Lee Y, Lee S, Park JW, et al. Hypoxia-induced neuroinflammation and learning–memory impairments in adult zebrafish are suppressed by glucosamine. *Mol Neurobiol*. 2018;55:8738-8753.
58. Taylor CT, Moncada S. Nitric oxide, cytochrome C oxidase, and the cellular response to hypoxia. *Arterioscler Thromb Vasc Biol*. 2010;30(4):643-647.

How to cite this article: Üstündağ ÜV, Ünal İ, Cansız D, et al. 520nm and 660nm light-emitting diodes modulates pancreatic development and beta cell functions in zebrafish embryos. *Photochem Photobiol*. 2025;101:1327-1342. doi:10.1111/php.14050